JOURNAL OF SOLID STATE CHEMISTRY 60, 305–315 (1985)

The Structure Tl_3SbS_3, Tl_3SbSe_3, $Tl_3SbS_{3-x}Se_x$, and $Tl_3Sb_yAs_{1-y}Se_3$

ARNE OLSEN,* PETER GOODMAN, AND HAROLD J. WHITFIELD

CSIRO, Division of Chemical Physics, Clayton, Victoria, Australia 3168

Received January 4, 1985; in revised form May 22, 1985

The space group symmetry and crystal structure of $Tl_3SbS_{3-x}Se_x$ compounds in the composition range $0 < x < 3$ have been determined by a combination of powder X-ray diffraction, electron diffraction, and high-resolution electron microscopy. The incongruently melting compound Tl_3SbSe_3 has been shown to crystallize in cubic space group $P2_13$ with $a = 9.435$ Å in a structure related to that of Langbeinite. The convergent beam electron diffraction pattern of Tl_3SbS_3 is in accord with the space group $R3m$ determined by X-ray diffraction. The cubic Langbeinite-type structure is found for $Tl_3SbS_{3-x}Se_x$ for $0.5 < x < 3$ and for $Tl_3Sb_yAs_{1-y}Se_3$ for $0.077 < y < 1.0$. A five-component compound $Tl_3Sb_{0.5}As_{0.5}Se_{1.5}S_{1.5}$ was also found to be cubic. © 1985 Academic Press, Inc.

Introduction

Tl_3AsS_3, Tl_3AsSe_3, Tl_3SbS_3, and Tl_3SbSe_3 are ternary chalcogenides of the large sulfosalt family. The thallium sulfosalts are of interest because of their nonlinear optical and acoustooptical properties. Thallium arsenic selenide has been suggested as a candidate for phase-matched second-harmonic generation and parametric oscillation applications. In addition thallium arsenic selenide has been used as an acoustooptic modulator, beam deflector, and tunable filter. The experimental and theoretical determination of the electronic structure of Tl_3AsSe_3 is the subject of a recent report (*1*). In searching for other compounds of similar structure and properties we have investigated the antimony analogues of these compounds, namely, Tl_3SbS_3, Tl_3SbSe_3, and $Tl_3SbS_{3-x}Se_x$.

Tl_3AsS_3, Tl_3AsSe_3, and Tl_3SbS_3 all crystallize in rhombohedral space group $R3m$ (*2–4*) with thallium and chalcogen atoms in special positions 9b (x $2x$ z) and arsenic or antimony atoms in special positions 3a ($0,0,z$). The values of the positional parameters for the three compounds are listed in Table I. The parameters for Tl_3AsS_3 have been transformed from the original rhombohedral to a hexagonal axial system. Comparison of the results suggests that the Se atom in Tl_3AsSe_3 has been misplaced up the z axis.

The compound Tl_3SbSe_3 has been reported previously (*5*) but not its crystal structure. In the present work a combination of powder X-ray diffraction, selected area and convergent beam electron diffraction, and high-resolution electron microscopy was found to be very useful in the determination of its structure. This was partly due to the fine-grained nature of the specimens but also partly due to the nature of the crystal structures.

* Permanent address Institute of Physics, University of Oslo, Oslo 3, Norway.

0022-4596/85 $3.00
Copyright © 1985 by Academic Press, Inc.
All rights of reproduction in any form reserved.

TABLE I

POSITIONAL PARAMETERS FOR Tl_3AsS_3 (*2*), Tl_3AsSe_3 (*3*), AND Tl_3SbS_3 (*4*)

		Tl_3AsS_3	Tl_3AsSe_3	Tl_3SbS_3
Tl	*x*	0.2044(5)	0.2052(1)	0.20524(7)
	y	0.4088(5)	0.4103(2)	0.41407(7)
	z	0.0000(4)	0.0	0.00000(4)
As	*x*	0.0000(7)	0.0	0.0
	y	0.0000(7)	0.0	0.0
	z	0.7543(7)	0.745 (1)	0.7572
S, Se	*x*	0.212 (2)	0.2052(4)	0.2037 (4)
	y	0.424 (2)	0.4103(8)	0.4074 (4)
	z	0.557 (2)	0.4480(9)	0.581 (1)

Experimental

Sample Preparation

Tl_3SbS_3, Tl_3SbSe_3, $Tl_3SbS_{3-x}Se_x$, $Tl_3As_{1-y}Sb_ySe_3$ and $Tl_3Sb_{0.5}As_{0.5}Se_{1.5}S_{1.5}$ were prepared by heating mixtures of thallium, pnicogen, and chalcogen in stoichiometric proportions in evacuated ampoules at 820 K for 2 hr. Cooled products were powdered and then annealed for 18 hr in evacuated ampoules just below the transition point of the sample. Crystals of Tl_3SbS_3 with sufficient size for examination by single-crystal X-ray diffraction were obtained. On the other hand attempts to grow single crystals of Tl_3SbSe_3 for X-ray work have been unsuccessful because it is an incongruently melting compound formed by a solid-state reaction.

X-Ray powder diffraction patterns of flat plate samples mixed with silver powder as internal standard were recorded on a Rigaku Miniflex X-ray diffractometer using Ni-filtered Cu radiation.

High-Resolution Microscopy (HREM) and Convergent Beam Diffraction (CBED)

Specimens suitable for electron microscopy were prepared by crushing the samples and placing the thin crystals on holey carbon films. High-resolution electron microscopy was carried out in a JEOL 200CX electron microscope equipped with a top entry goniometer stage. The microscope had a LaB_6 filament and a double gap first condensor. Images were recorded at a magnification of 850,000. The top-entry stage goniometer allowed the specimen to be tilted ± 10 about two orthogonal axes. The spherical aberration constant C_s of the objective lens was improved from 1.2 to 0.94 mm by placing the specimen very low in the objective. The value of C_s has been determined by optical diffractograms of amorphous Ge films (*6*) and was confirmed by image matching of known structures with large unit cells. The chromatic aberration constant, C_c has previously been determined by the same image matching technique and found to be consistent with 1.2 mm. The incident beam divergence used for imaging was 8×10^{-4} rad or less.

Convergent beam electron diffraction (CBED) patterns were taken in a convergent beam camera of a modified Siemens Elmiscope I, with a liquid-nitrogen-cooled specimen goniometer (*7*).

Results

Tl_3SbS_3

X-Ray precession photographs of a single crystal of Tl_3SbS_3 showed it belongs to rhombohedral space group with systematic absences observed from *hk*0, *hk*1, *hk*2, and *hhl* precession photographs for $h + k + l$ not equal to $3n$. This condition was also found in single crystal selected area electron diffraction patterns. The space groups allowed from these systematic absences are $R3m$, $R\bar{3}m$, $R32$, $R3$, and $R\bar{3}$.

The [0001] CBED pattern taken in the cooled stage of the Elmiskop I is shown in Fig. 1. This pattern shows a strong trigonal symmetry with the projected symmetry of $P31m$ (planar group No. 14) rather than $P3m1$ (planar group No. 13). Only $R3m$ (No. 166) is consistent with this projected

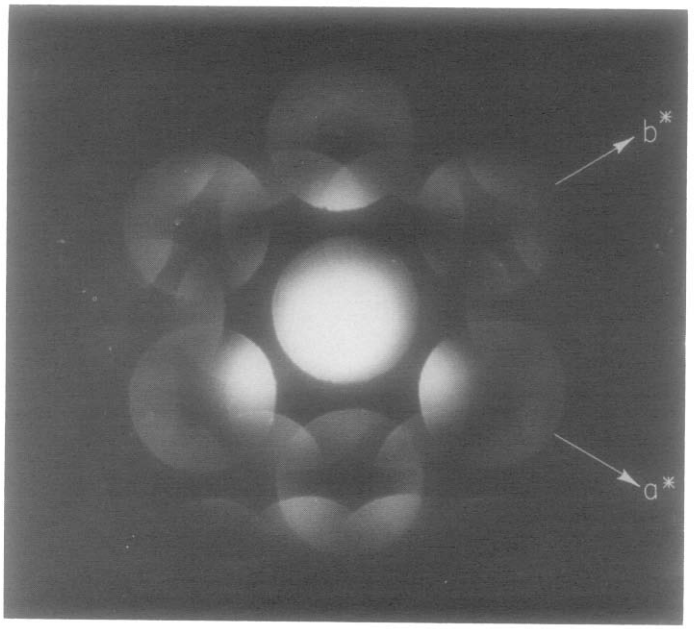

FIG. 1. CBED pattern of Tl_3SbS_3 in [001] orientation.

zone axis symmetry and with the above X-ray absences, $R32$, $R3$, and $R\bar{3}$ having no mirror symmetries while $R\bar{3}$ can result in trigonal zone-axis symmetries only through upper layer interactions. In projection this latter space group has six rather than three mirror lines. Zone axis patterns displaying simple zero-order diffraction distributions of circular rather than trigonal character, cannot reasonably have a strong upper-layer influence on their diffracted symmetries (*8*).

This conclusion from the CBED pattern is in good accord with the structure refinement based on single crystal X-ray data (*4*). Also the point symmetry at 3(a) position of $R3m$ is $3m$ so that an asymmetry parameter of zero is predicted for the Sb nuclear quadrupole resonance in accord with the experimental observation (*5*).

Tl_3SbSe_3

The X-ray powder diffraction pattern could be indexed in terms of a cubic cell with $a = 9.435$ Å (Table II). A microcrystal-

TABLE II

X-RAY POWDER PATTERN OF Tl_3SbSe_3

hkl	d_{calc}	d_{obs}	I_{obs}	I_{calc}
011	6.672	6.68	1	5
111	5.447	5.44	2	1
012, 021	4.219	4.21	7	4
112	3.852	3.85	16	22
022	3.356	3.34	33	37
122	3.145	3.14	6	5
013, 031	2.984	2.98	100	100
113	2.845	2.84	10	3
222	2.724	2.72	5	3
023, 032	2.617	2.61	13	3
123, 132	2.522	2.52	60	55
033, 114	2.224	2.22	2	1.2
133	2.165	2.17	3	1.1
024, 042	2.110	2.11	4	0.8
124, 142	2.059	2.06	6	0.3
233	2.012	2.01	7	6
224	1.926	1.926	17	13
015, 051, 134, 143	1.850	1.850	34	41
333	1.816	1.818	6	0.1
025, 052, 234, 243	1.752	1.753	4	0.5
125, 152	1.723	1.722	10	11

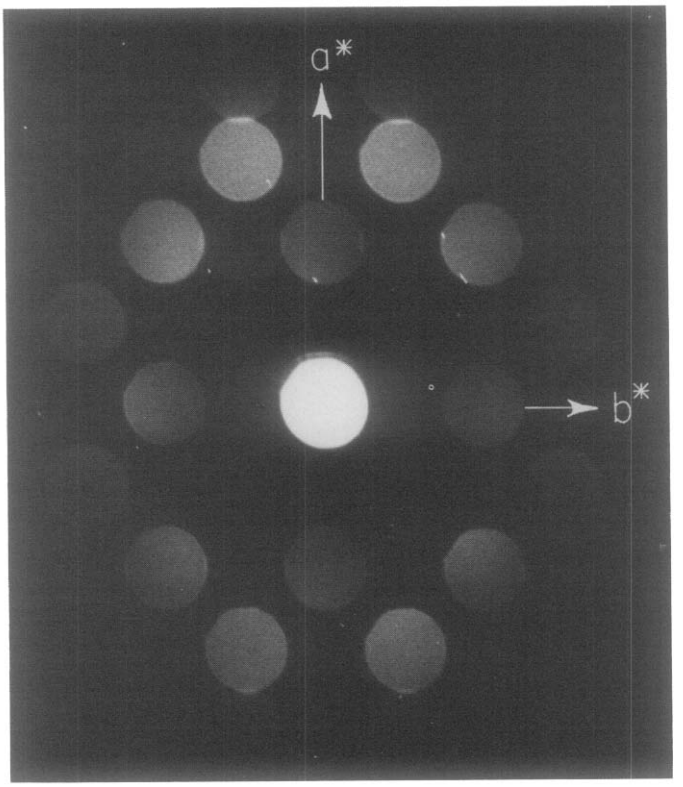

FIG. 2. CBED pattern of Tl_3SbSe_3 in [001] orientation.

line powder was found to be sufficiently stable in the electron beam of the JEOL 200 CX microscope and electron diffraction patterns and lattice images were recorded. The selected area electron diffraction patterns and high-resolution lattice images are consistent with cubic space group symmetry. CBED patterns taken in the Elmiscop 1 diffraction camera, at the [001] zone axis setting showed a square lattice having only 2-fold symmetry as shown in Fig. 2. This pattern shows extinction along both axes for $h \neq 2n$ or $k \neq 2n$. Again, assuming that the projection approximation is valid from the appearance of the central beam, the projected space group is *pgg*. This rules out all 4-fold symmetric groups of the cubic system. Taken together with the extinctions this data uniquely determines the space group as $P2_13$ (No 198). A value of $Z = 4$ gives a calculated density $d_{calc} = 9.046$ g cm^{-3}. Various model structures were constructed of which only one was found to account even qualitatively for the X-ray powder intensities. This trial structure had three Tl atoms and one Sb atom in special positions 4a of the space group and one Se atoms in a 12-fold general position 12b. The approximate coordinates of this Se were (0.25, 0.25, 0) from packing and coordination considerations. Because of the overlap of nonequivalent reflections in a powder X-ray pattern the coordinates of the Se atom in a general position could not be determined. We therefore used single crystal information from CBED to locate the Se atom and refine the structure. In the CBED pattern of Fig. 2 the departure from 4-fold symmetry is clearly evident. For example the pairs of reflections 310,130 and 410,140

TABLE III

POSITIONAL PARAMETERS

	x	y	z
	(a) Tl_3SbSe_3		
Tl(1)	0.0625	0.0625	0.0625
Tl(2)	0.5625	0.5625	0.5625
Tl(3)	0.310	0.310	0.310
Sb	0.8125	0.8125	0.8125
Se	0.668	0.433	0.284
	(b) $K_2Mg_2(SO_4)_3$		
K(1)	0.068	0.068	0.068
Mg(1)	0.584	0.584	0.584
K(2)	0.297	0.297	0.297
Mg(2)	0.850	0.850	0.850
S	0.625	0.467	0.268

have markedly different intensities. N-beam dynamical intensities for the electron scattering were calculated as a function of crystal thickness for different atomic positions of Tl, Sb, and Se. As initial trial structure the coordinates obtained from fitting X-ray powder data were taken. Calculated intensities were compared with the experimental data of Fig. 2. The crystal thickness could be determined from the strongest reflections whereas the extent of deviation from 4-fold symmetry was determined by comparing for example the pairs of reflections 310,130 and 410,140. As the crystal was wedge-shaped it was necessary to integrate calculated intensities over a thickness range. Satisfactory agreement between calculated and observed relative intensities was found for the atomic positions listed in TABLE IIIa. The intensities were integrated over a thickness range 94 to 132 Å. Examples of the pendellosung calculations of the nonequivalent reflections 130,310, 410,140, and 230,320 as well as reflections 020,220 are shown in Fig. 3.

Using the atom coordinates of the refined structure, X-ray intensities I_{hkl} were calculated from the relationship $I_{hkl} = MLPF^2_{khl}$ where M, is the multiplicity, L the Lorentz factor, P the polarization, and F_{hkl} the calculated structure factor for the reflection. In calculating the structure factors isotropic temperature factors found for Tl_3SbS_3 were used. The agreement between calculated and observed intensities of X-ray powder

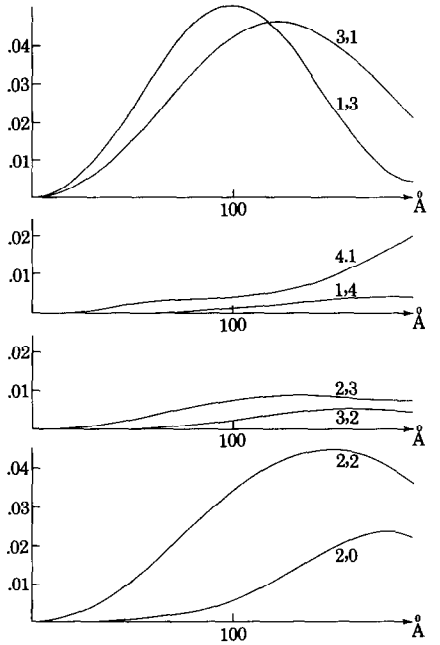

FIG. 3. N-beam calculation of pendellosung of 130, 310, 410 and 140 beams of Tl_3SbSe_3 in [001] orientation.

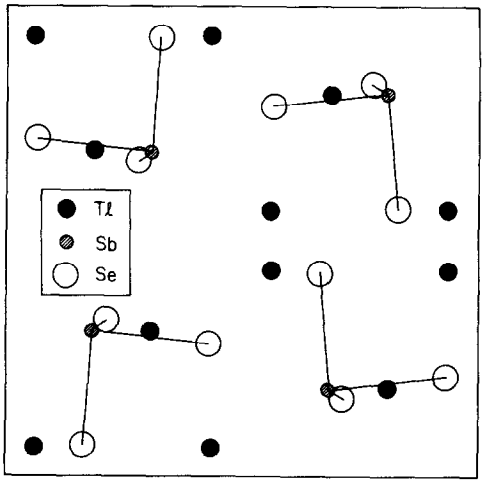

FIG. 4. Projection of the structure of Tl_3SbSe_3 down [001].

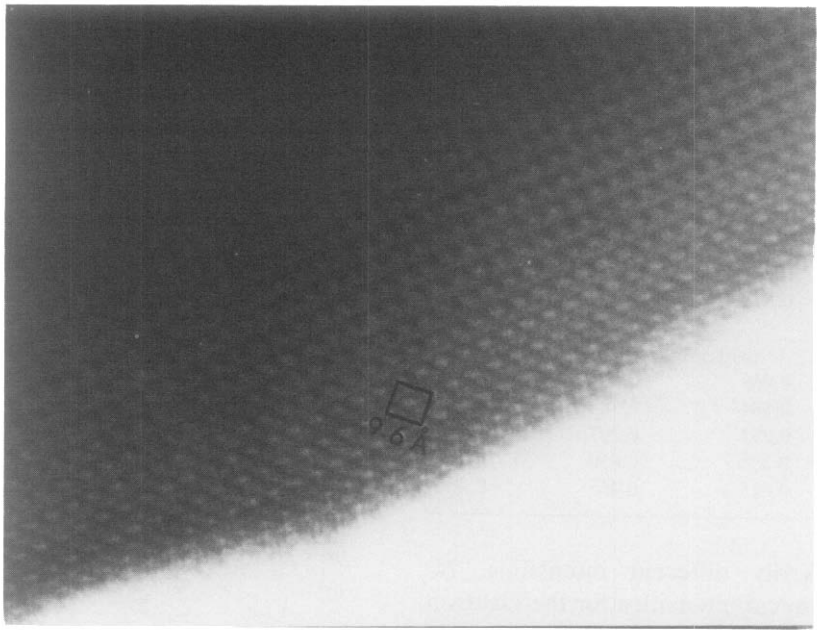

FIG. 5. Lattice image of Tl_3SbSe_3 in [001] orientation.

diffraction peaks (Table II) is confirmation of the proposed structure.

The proposed structure is shown in Fig. 4 and HREM in Fig. 5. For Sb in position 4a the point group symmetry at the Sb site is 3 and a zero asymmetry parameter is predicted for the Sb nuclear quadrupole resonance in accord with experiment (*5*). Further confirmation of the proposed structure Tl_3SbSe_3 was obtained by matching experimental and computed lattice images. Specimens in the [001] orientation were difficult to prepare by crushing and the successful samples were obtained by grinding at 77 K. The images produced from the crystals in this orientation were of indifferent quality. However, preferred cleavage on (112) produced far better samples for high-resolution electron microscopy. Figure 6 shows the [112] projection of the proposed structure of Tl_3SbSe_3. In this orientation the Tl atoms form large tunnels which give rise to high contrast in the lattice images (Fig. 7). Due to the large differences in scattering factor for Tl, Sb, and Se the major contribution to the image contrast arises from the Tl and Sb atoms.

High-resolution lattice images were calculated using the multislice formulation of the dynamical theory for electron diffraction (*9, 10*). The calculations were carried out using a special purpose computer program of D. Lynch. Atomic scattering fac-

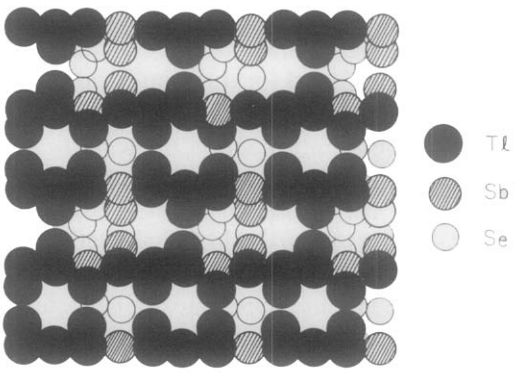

FIG. 6. Projection of the structure of Tl_3SbSe_3 down [112].

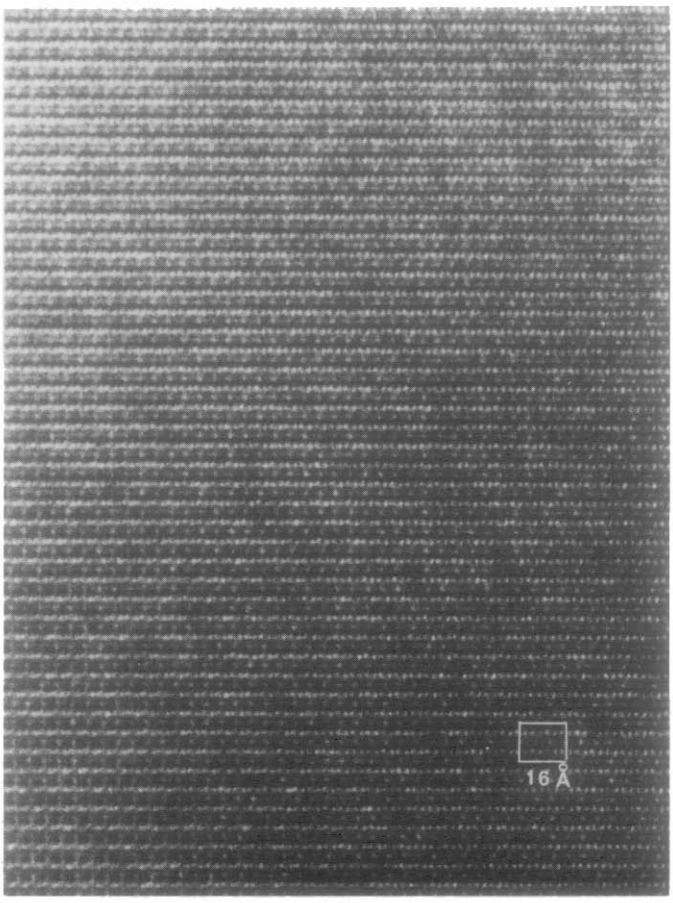

FIG. 7. Lattice images of Tl_3SbSe_3 [112] projection.

tors were taken from Cromer and Waber (*11*). The best agreement between calculated and experimental images was found to occur near −600 Å defocus. At this electron optical condition the effect of beam divergence of the incident electron beam and chromatic aberration could in many cases be simulated by using an effective objective aperture with radius 2.0 Å. The experimental image in Fig. 7 is in good agreement with the projected potential of the proposed structure (Fig. 8a) and with the calculated lattice image (Fig. 8b) which shows that the bright parts in the experimental image of Fig. 7 correspond to tunnels in the structure.

$Tl_3SbS_{3-x}Se_x$ and $Tl_3Sb_yAs_{1-y}Se_3$

Mixed chalcogenides $Tl_3SbS_{3-x}Se_x$ with x values 0.3, 0.6, and 1.0 and mixed arsenic and antimony compositions $Tl_3Sb_yAs_{1-y}Se_3$ with y values 0.05, 0.077, 0.1, and 0.5 were examined by X-ray powder diffraction. In all cases the diffraction patterns could be indexed in terms of hexagonal or cubic unit cells of dimensions listed in Table IV. The linear plot of lattice dimension against composition (Fig. 9) indicates the existence of a range of substitutional solid solution. No two-phase region of $R3m$ and $P2_13$ structures was detected. The X-ray powder pattern of the five-component compound

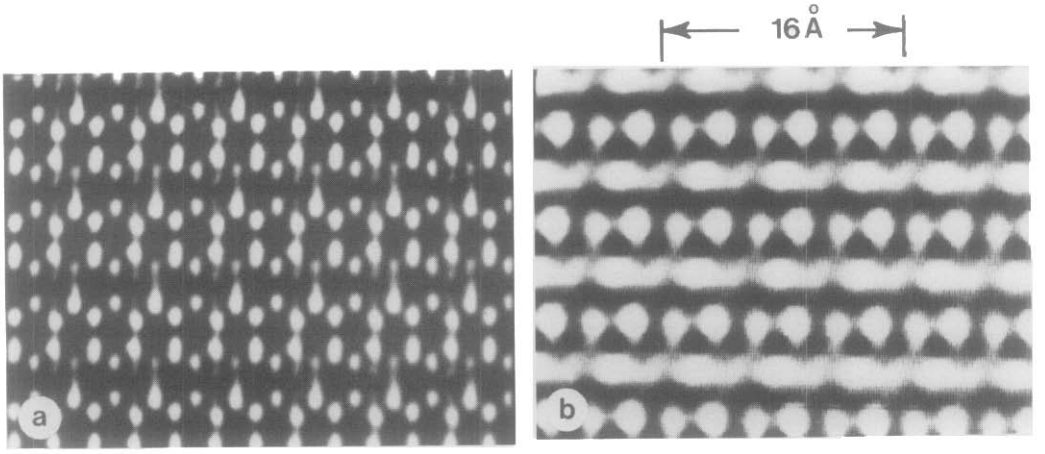

FIG. 8. (a) Projected potential of Tl_3SbSe_3 down [112]; (b) calculated lattice image of Tl_3SbSe_3 down [112] at a defect of focus 500 Å for 46-Å thick crystal.

$Tl_3Sb_{0.5}As_{0.5}Se_{1.5}S_{1.5}$ was also consistent with the cubic structure.

Discussion of the Structures

The structure of Tl_3SbS_3 (space group *R*3*m*) is very similar to the structure of pyrargyrite Ag_3SbS_3 with space group *R*3*c*. Both structures have some similarities to the structure of the cubic Tl_3SbSe_3. The Figs. 10a and b shows the structures of Tl_3SbS_3 and Ag_3SbS_3 projected along the rhombohedral *c* axis. Data for pyrargyrite, Ag_3SbS_3, were taken from Harker (*12*). The space group is rhombohedral *R*3*c* and the hexagonal unit cell dimensions are a = 11.06 Å and c = 8.73 Å. Fig. 10c shows the

TABLE IV

SPACE GROUP AND CELL DIMENSIONS OF SOLID SOLUTIONS

		Cell dimensions	
x	S G	a (Å)	c (Å)
	$Tl_3SbS_{3-x}Se_x$		
0.0	*R*3*m*	9.519	7.36
0.3	*R*3*m*	9.540	7.38
0.6	$P2_13$	9.25_0	
1.0	$P2_13$	9.27_0	
3.0	$P2_13$	9.43_5	
	$Tl_3Sb_yAs_{1-y}Se_3$		
0.00	*R*3*m*	9.87_0	7.09_4
0.5	*R*3*m*	9.88_0	7.10_5
0.077	*R*3*m*	9.89_5	7.11_0
0.077	$P2_13$	9.33_0	
0.10	$P2_13$	9.33_1	
0.50	$P2_13$	9.375	
1.00	$P2_13$	9.43_5	

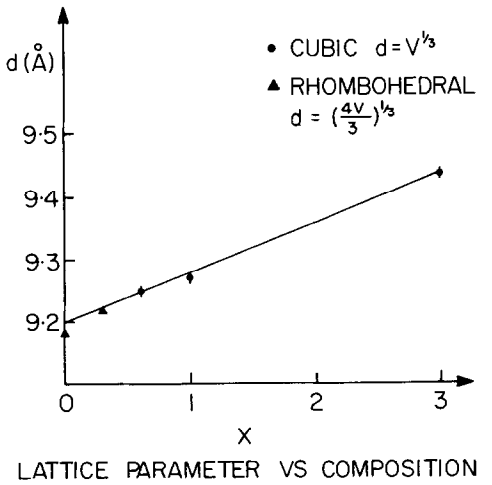

FIG. 9. Graph of lattice parameter vs composition for $Tl_3SbS_{3-x}Se_x$

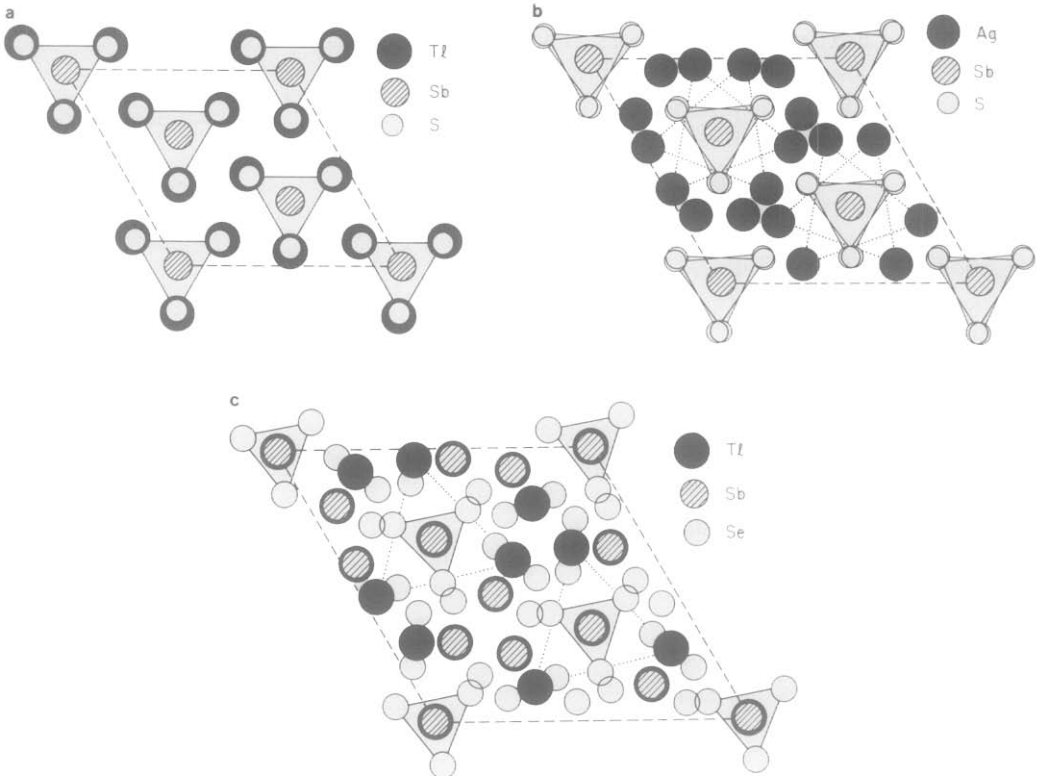

FIG. 10. Comparison of the structures of (a) Tl_3SbS_3, (b) Ag_3SbS_3, and (c) Tl_3SbSe_3.

structure of Tl_3SbSe_3 projected along the [111] direction.

All the three structures in Fig. 10 contain Sb atoms coordinated to a triangle of chalcogenide atoms with the Sb displaced from the center perpendicular to the hexagonal a, b plane in Tl_3SbS_3 and Ag_3SbS_3 and to (111) planes in Tl_3SbSe_3. In the rhombohedral $R3m$ and $R3c$ structures these triangles form spirals about the c axis whereas in the cubic Tl_3SbSe_3 structure with space group $P2_13$ these triangles form spirals about the $\langle 111 \rangle$ axes. In the Tl_3SbS_3 structure there is another spiral formed by equilateral triangles of Tl atoms at a distance of approximately $0.56c$ beneath the S triangles. There is no metal atom chain along the spiral axis. In the Ag_3SbS_3 ($R3c$) structure the SbS_3 pyramidal groups form a spiral with a complete turn of 2π equivalent to a translation along c of 8.73 Å. Near the spiral axis there is another spiral formed by a chain of Tl atoms. These two spirals are of opposite direction. In the Tl_3SbSe_3 ($P2_13$) structure $SbSe_3$ pryamidal groups form spirals with the spiral axes along the four different $\langle 111 \rangle$ directions. The periodicity of these helixes is equal to $a \cdot \sqrt{3}$, that is, 16.34 Å. Near the center of these spirals there are three other spirals running in the same direction. Two are formed by Tl and Sb atoms with the Sb atoms $\frac{1}{2} \cdot \sqrt{3} \cdot a$ below the Tl atoms. The third spiral is formed by Se atoms. Tables V and VI show selected interatomic distances angles and coordination number for Tl_3SbS_3 and Tl_3SbSe_3.

In Tl_3SbS_3 each thallium atoms is surrounded by five S atoms two at a distance of 3.00 Å, one at 3.08 Å and two at 3.64 Å. On the other hand in Tl_3SbSe_3 each Tl atom

is surrounded by six Se atoms; three nearest and three next-nearest neighbors. The shortest Tl–Sb bond distance in Tl_3SbSe_3 is 3.74 Å compared to 3.77 Å in Tl_3SbS_3. Each Sb atoms in Tl_3SbSe_3 is surrounded by three Se and three Tl atoms at a distance of 2.3 and 3.74 Å, respectively. In Tl_3SbS_3 the Sb atoms have three S atoms as nearest neighbors at a distance of 2.43 Å and the next-nearest neighbours are three sulfur atoms at 3.60 Å.

A comparison of the atomic positions for the Tl_3SbSe_3 structure with those for the Langbeinite $K_2Mg_2(SO_4)_3$ structure (*13*) shows remarkable but unexplained similarities as seen in Table IIIb.

The refinement of the position of the Se atoms in based on the convergent beam electron diffraction data and its estimated standard deviation is of order 0.1 Å, whereas the estimated standard deviations of the thallium and antimony positions based on both the X-ray powder diffraction intensities and on the lattice images are of order 0.02 Å. Comparison with other structures suggest that the values determined for the Se–Sb–Se and the Sb–Se bonds are almost certainly too low compared to the S–Sb–S angle and the Sb–S bond. The selenium atom positions could be most readily refined by single crystal X-ray data and we are attempting to grow single crystals of Tl_3SbSe_3 for this purpose.

TABLE V

SELECTED INTERATOMIC DISTANCES (Å) AND ANGLE Se–Sb–Se IN Tl_3SbSe_3

Tl(1) Coordination	
Tl(1)–Se	3.17, 3.42
Tl(1)–Sb	4.09
Tl(1)–Tl(2)	3.73
Tl(1)–Tl(3)	4.04
Tl(2) Coordination	
Tl(2)–Se	3.06, 3.29
Tl(2)–Sb	4.09
Tl(2)–Tl(1)	3.73
Tl(2)–Tl(2)	4.13
Tl(3) Coordination	
Tl(3)–Se	3.58, 3.67
Tl(3)–Sb	3.74
Tl(3)–Tl(1)	4.04
Tl(3)–Tl(2)	4.13
Sb Coordination	
Sb–Be	2.34, 4.22
Sb–Tl(3)	3.74
Sb–Tl(1)	4.09
Sb–Tl(2)	4.09
Se–Sb–Se	88.5
Se Coordination	
Se–Se	3.26
Se–Sb	2.34
Se–Tl(1)	3.17, 3.42
Se–Tl(2)	3.06, 3.29
Se–Tl(3)	3.58, 3.67

TABLE VI

SELECTED INTERATOMIC DISTANCES (Å) AND S–Sb–S ANGLE FOR Tl_3SbS_3

Tl Coordination	
Tl–S	3.00, 3.08, 3.46
Tl–Sb	3.77, 3.83
Tl–Tl	3.66, 3.85
Sb Coordination	
Sb–S	2.43, 3.60
Sb–Tl	3.77, 3.83
S–Sb–S	99.2
S Coordination	
S–S	3.70, 3.83
S–Sb	2.43, 3.60
S–Tl	3.00, 3.08, 3.46

Conclusion

The structure of Tl_3SbSe_3 for which only microcrystals have been prepared was solved by a combination of X-ray powder and convergence beam electron diffraction and confirmed by high-resolution electron microscopy. Tl_3SbS_3 was confirmed to be isostructural with Tl_3AsS_3 and Tl_3AsSe_3. The stability range of the Tl_3SbSe_3 structure on substituting S for Se or As or As for Sb has been determined.

References

1. M. D. EWBANK, S. P. KOWALCZYK, E. A. KRAUT, AND W. A. HARRISON, *Phys. Rev. B* **24,** 926 (1981).
2. M. GOSTOJIC, *Z. Kristallogr.* **151,** 249 (1980).
3. H, Y-P, HONG, J. C. MIKKELSEN, AND G. W. ROLAND, *Mat. Res. Bull.* **9,** 365 (1974).
4. N. REY, J. C. JUMAS, J. OLIVIER-FOURCADE, AND E. PHILIPPOT, *Acta Crystallogr. C* **40,** 1655 (1984).
5. T. J. BASTOW AND H. J. WHITFIELD, *J. Solid State Chem.* **40,** 203 (1981).
6. S. R. GLANVILL, A. F. MOODIE, H. J. WHITFIELD, AND I. J. WILSON, *Aust. J. Phys.*, in press.
7. W. C. T. DOWELL AND D. WILLIAMS, *Ultramicroscopy* **1,** 43 (1976).
8. P. GOODMAN, "Electron Diffraction 1927–1977" (P. J. Dobson, Ed.), Inst. Physics Conf. Ser. No 41, p. 116, Inst. Phys., Bristol (1978).
9. J. M. COWLEY AND A. F. MOODIE, *Acta Crystallogr.* **10,** 609 (1957).
10. P. GOODMAN AND A. F. MOODIE, *Acta Crystallogr. A* **30,** 280 (1974).
11. D. T. CROMER AND J. T. WABER, *Acta Crystallogr.* **18,** 104 (1965).
12. D. HARKER, *J. Chem. Phys.* **4,** 381 (1936).
13. A. ZEMANN AND J. ZEMANN, *Acta Crystallogr.* **10,** 409 (1957).